Letter

$\mathbb{C}P^2$ skyrmion crystals in an SU(3) magnet with a generalized Dzyaloshinskii-Moriya interaction

Yuki Amari [1,2,3,4,5] Yutaka Akagi [1] Sven Bjarke Gudnason [6] Muneto Nitta [5,7] and Yakov Shnir [2,8]

[1]*Department of Physics, Graduate School of Science, The University of Tokyo, Bunkyo, Tokyo 113-0033, Japan*
[2]*Bogoliubov Laboratory of Theoretical Physics, Joint Institute for Nuclear Research, Dubna 141980, Moscow Region, Russia*
[3]*Department of Physics, Faculty of Science and Technology, Tokyo University of Science, Noda, Chiba 278-8510, Japan*
[4]*Department of Mathematical Physics, Toyama Prefectural University, Kurokawa 5180, Imizu, Toyama 939-0398, Japan*
[5]*Research and Education Center for Natural Sciences, Keio University, Hiyoshi 4-1-1, Yokohama, Kanagawa 223-8521, Japan*
[6]*Institute of Contemporary Mathematics, School of Mathematics and Statistics, Henan University, Kaifeng, Henan 475004, People's Republic of China*
[7]*Department of Physics, Keio University, Hiyoshi 4-1-1, Yokohama, Kanagawa 223-8521, Japan*
[8]*Institute of Physics, University of Oldenburg, D-26111 Oldenburg, Germany*

(Received 16 April 2022; revised 3 August 2022; accepted 30 August 2022; published 19 September 2022)

We study $\mathbb{C}P^2$ skyrmion crystals in the ferromagnetic SU(3) Heisenberg model with a generalization of the Dzyaloshinskii-Moriya interaction and the Zeeman term. The model possesses two different types of skyrmion crystals with unit skyrmions that can be interpreted as bound states of two half-skyrmions or four quarter-skyrmions. Our study on $\mathbb{C}P^2$ skyrmion crystals opens up the possibility for useful future applications since $\mathbb{C}P^2$ skyrmions have more degrees of freedom than the usual $\mathbb{C}P^1$ (magnetic) skyrmions.

DOI: 10.1103/PhysRevB.106.L100406

I. INTRODUCTION

Skyrmions in their original incarnation were invented by Skyrme as a simple topological model of nuclei [1], but were first taken more seriously after Witten showed that they are the baryons of large-N_c quantum chromodynamics (QCD) [2] and have led to many qualitative results [3,4]. Insights for the interactions of skyrmions at large separations were subsequently found in a two-dimensional toy model, called the baby-Skyrme model [5–7]. Recently, similar topological structures known as magnetic skyrmions [8,9] have received quite intensive focus due to their realizations in the laboratory in chiral [10–12] or noncentrosymmetric [13–16] magnets and their possible applications as components for data storage with low-energy consumption [17] (see Ref. [18] for a review).

Skyrmions in two-dimensional materials are topological solitons with the target of a 2-sphere, which is parametrized by a magnetization vector of fixed length. The topological charge or degree comes from considering only finite-energy configurations, which forces the magnetization vector to be a constant at asymptotic distances and therefore the topology is that of maps between two spheres: $\pi_2(S^2) = \mathbb{Z} \ni N$. Nontrivial topology, however, does not ensure that skyrmions are actually realizable in a material. It is also necessary that there is some stabilizing mechanism at work. Skyrmions in chiral magnets are stabilized by the Dzyaloshinskii-Moriya (DM) interaction term—stemming from spin-orbit coupling (SOC)—which stabilizes skyrmions with one chirality, but not the other. Skyrmions in chiral magnets have a fixed vector chirality [10], whereas this is a degree of freedom in noncentrosymmetric materials and the stabilizing mechanism at work is also different. In the latter materials, the stabilization of skyrmions is due to frustration, magnetic anisotropy [19–21], and multiple-spin interactions mediated by itinerant electrons [22–24], instead of the DM term.

A two-dimensional sphere (S^2) can also be viewed as a complex projective plane ($\mathbb{C}P^1$). Although planar skyrmions cannot be topologically stable with higher-dimensional spheres S^n, $n > 2$, for their target space, they can be topological for $\mathbb{C}P^n$ with $n \geqslant 1$. The $\mathbb{C}P^n$ model was proposed about half a century ago [25–27] and has been studied in quantum field theory, as the (1+1)-dimensional $\mathbb{C}P^n$ model shares various properties with (3+1)-dimensional gauge theories, such as a dynamical mass gap, asymptotic freedom, and instantons (spacetime analogs of planar skyrmions) [28,29]. In condensed matter physics, the $\mathbb{C}P^n$ model has been studied for a new quantum phase transition called deconfined criticality [30,31], and proposed to be realized in ultracold atomic gases [32], multiband superconductors [33–35], and $S = 1$ spin systems [36–42] where solitons (skyrmions) [43–47] and vortices [43,48–52] can emerge. A physically relevant and interesting minimal extension is the case of the $\mathbb{C}P^2$ target space, which appears as the order parameter space of an effective model of the spin-1 Bose-Hubbard model [45,53]. In addition, an SU(3) SOC can be induced by applying a laser beam to ultracold atomic gases [54–58]. Therefore, ultracold atom systems offer a promising candidate to realize $\mathbb{C}P^2$ skyrmions.

Skyrmions realized in nature are often in the form of crystals. Skyrmion crystals were first considered in the three-dimensional Skyrme model [59,60] and at finite (large) density, there is a transition from unit skyrmions to half-skyrmions [61]. Arrays or crystals of magnetic skyrmions for normal $\mathbb{C}P^1$ skyrmions are also realized in magnets [10–16]. On the other hand, such magnetic skyrmion crystals have been considered in classical spin systems or $\mathbb{C}P^1$ magnets. Since skyrmions with $\mathbb{C}P^2$ target space are also topological,

but have more internal structure, the realization of a $\mathbb{C}P^2$ skyrmion crystal in some material may have useful future applications.

The purpose of this Letter is to propose the possibility of skyrmion crystals with the degrees of freedom of $\mathbb{C}P^2$. We find that there are two different crystal types, depending on a single free parameter. The parameter has to be small enough (below a critical value) for the skyrmions to exist and not be energetically disfavorable to the ferromagnetic phase.

II. MODEL

We consider a low-energy effective Hamiltonian of the spin-1 Bose-Hubbard model with an SU(3) SOC on a square lattice [62]. Let $\hat{S}_i^a$ $(a = x, y, z)$ and $\hat{T}_i^\alpha$ $(\alpha = 1, 2, \ldots, 8)$ be the spin-1 and SU(3) spin operators defined on site i, respectively. In terms of the operators, the Hamiltonian is given by

$$\hat{H} = \hat{H}_{\mathrm{SU(3)}} + \hat{H}_{\mathrm{DM}} + \hat{H}_{\mathrm{Zeeman}}, \tag{1}$$

$$\hat{H}_{\mathrm{SU(3)}} = \frac{J}{2}\sum_{\langle i,j\rangle}\sum_{\alpha=1}^{8}\hat{T}_i^\alpha\hat{T}_j^\alpha, \tag{2}$$

$$\hat{H}_{\mathrm{DM}} = J\sum_{\langle i,j\rangle}\sum_{\alpha,\beta,\gamma=1}^{8} f_{\alpha\beta\gamma}A_{i,j}^\alpha\hat{T}_i^\beta\hat{T}_j^\gamma, \tag{3}$$

$$\hat{H}_{\mathrm{Zeeman}} = -h\sum_i \hat{S}_i^z, \tag{4}$$

where $\hat{H}_{\mathrm{SU(3)}}$, $\hat{H}_{\mathrm{DM}}$, and $\hat{H}_{\mathrm{Zeeman}}$ are the ferromagnetic SU(3) Heisenberg term $(J < 0)$, the generalized DM interaction term [63], and the Zeeman interaction, respectively. Here, the sum $\langle i, j\rangle$ is taken over the nearest-neighbor sites, $f_{\alpha\beta\gamma}$ are the structure constants of SU(3) defined as $f_{\alpha\beta\gamma} = -\frac{i}{4}\,\mathrm{Tr}(\lambda_\alpha[\lambda_\beta, \lambda_\gamma])$ where λ_α $(\alpha = 1, 2, \ldots, 8)$ are the Gell-Mann matrices, and $A_{i,j}^\alpha = \frac{1}{2}\,\mathrm{Tr}(\lambda_\alpha A_{i,j})$ is the SU(3) gauge potential. The SU(3) spin operator can be written as a product of spin-1 operators, and inversely spin-1 operators can be defined by SU(3) spin operators. In this Letter, we use the defined defining the spin-1 operators as

$$\hat{\mathbf{S}}_i = \left(\frac{\hat{T}_i^1 + \hat{T}_i^6}{\sqrt{2}}, \frac{\hat{T}_i^2 + \hat{T}_i^7}{\sqrt{2}}, \frac{\hat{T}_i^3 + \sqrt{3}\hat{T}_i^8}{2}\right). \tag{5}$$

To study skyrmion crystals in this model, we employ the variational approach with an SU(3) coherent state,

$$|\mathbf{Z}\rangle = \otimes_i|\mathbf{Z}_i\rangle, \quad |\mathbf{Z}_i\rangle = Z_i^m|m\rangle_i \quad \text{such that} \quad \mathbf{Z}_i^\dagger\mathbf{Z}_i = 1. \tag{6}$$

Here, $|m\rangle_i \equiv |S = 1, m\rangle_i$ $(m = 0, \pm 1)$ are the eigenstates of $\hat{S}_i^z$, and $\mathbf{Z}_i = (Z_i^1, Z_i^0, Z_i^{-1})^T$. The state represents an arbitrary spin-1 state. The classical Hamiltonian to be minimized is given by the expectation value of the quantum Hamiltonian (1) in the coherent state,

$$\begin{aligned} H &= \langle\mathbf{Z}|\hat{H}|\mathbf{Z}\rangle \\ &= \frac{J}{2}\sum_{\langle i,j\rangle}\left[\sum_{\alpha=1}^{8} n_i^\alpha n_j^\alpha + \sum_{\alpha,\beta,\gamma=1}^{8} 2f_{\alpha\beta\gamma}A_{i,j}^\alpha n_i^\beta n_j^\gamma\right] \\ &\quad - \frac{h}{2}\sum_i\left(n_i^3 + \sqrt{3}n_i^8\right), \end{aligned} \tag{7}$$

where the field n_i^α is the expectation value of the SU(3) spin operator on the lattice site i defined as

$$n_i^\alpha = \mathbf{Z}_i^\dagger\lambda_\alpha\mathbf{Z}_i. \tag{8}$$

The field n_i^α satisfies

$$\sum_{\alpha=1}^{8} n_i^\alpha n_i^\alpha = \frac{4}{3}, \quad \sum_{\alpha,\beta=1}^{8} d_{\alpha\beta\gamma}n_i^\alpha n_i^\beta = \frac{3}{2}n_i^\gamma, \tag{9}$$

where $d_{\alpha\beta\gamma} = \frac{1}{4}\,\mathrm{Tr}(\lambda_\alpha, \{\lambda_\beta, \lambda_\gamma\})$ are the symmetric symbols of SU(3).

For the SU(3) gauge potential $A_{i,j}$, we use the form

$$A_{i,i\pm\hat{x}} = \pm\frac{\kappa}{J}(\lambda_1 + \lambda_6), \quad A_{i,i\pm\hat{y}} = \pm\frac{\kappa}{J}(\lambda_2 + \lambda_7), \tag{10}$$

where $\hat{x}$ and $\hat{y}$ denote the bond vectors of the length of the lattice spacing, and κ is a constant. The SU(3) SOC with Eq. (10) can be recognized as a generalization of the Rashba SOC, which can be engineered in cold atom systems [54,64].

Skyrmions are topological solitons with an integer topological charge that is the degree of the map from two-dimensional space $\mathbb{R}^2$ to the $\mathbb{C}P^2$ target space: $\pi_2(\mathbb{C}P^2) = \mathbb{Z} \ni N$. The topological charge N can be computed by integrating the topological charge density

$$N = \frac{i}{32\pi}\int d^2x\,\epsilon_{jk}\,\mathrm{Tr}(\mathfrak{n}[\partial_j\mathfrak{n}, \partial_k\mathfrak{n}]), \tag{11}$$

with the color field $\mathfrak{n} = \sum_{\alpha=1}^{8} n^\alpha\lambda_\alpha$, for a continuous limit of the field n_i^α. In the lattice model, the topological charge density is analogously given by $N = \sum_i N_i$ with

$$N_i = -\frac{1}{16\pi}\sum_{\alpha,\beta,\gamma=1}^{8} f_{\alpha\beta\gamma}n_i^\alpha\left(n_{i+\hat{x}}^\beta - n_{i-\hat{x}}^\beta\right)\left(n_{i+\hat{y}}^\gamma - n_{i-\hat{y}}^\gamma\right). \tag{12}$$

The topological charge density N_i can also be interpreted as the SU(3) scalar spin chirality.

In this Letter, we set $J = -1$ without loss of generality. In addition, for studying long-wavelength excitations such as skyrmions, it is reasonable to fix one more parameter, because if we take the continuum limit, we can scale away two coupling constants. Therefore, we here fix $\kappa = 0.2$ and let h be the free parameter.

A. Numerical method

Our numerical method is described as follows. We first perform the minimization of the Hamiltonian (7) with periodic boundary conditions using an unbiased, single-update simulated annealing method with randomly generated initial configurations, increasing the inverse temperature β by a factor of 1.01 at every 10^4–10^5 Monte Carlo steps, until β reaches $\beta^{\max} \sim 10^2$–10^4. After that, we use the nonlinear conjugate gradients method to solve the equations of motion

$$\begin{aligned} \frac{\partial n_i^\alpha}{\partial\,\mathrm{Re}\,Z_i^m}\frac{\partial H}{\partial n_i^\alpha} - \omega_i\,\mathrm{Re}\,Z_i^m &= 0, \\ \frac{\partial n_i^\alpha}{\partial\,\mathrm{Im}\,Z_i^m}\frac{\partial H}{\partial n_i^\alpha} - \omega_i\,\mathrm{Im}\,Z_i^m &= 0, \end{aligned} \tag{13}$$

to obtain configurations with precise energies. The parameters ω_i are Lagrange multipliers at each lattice site i.

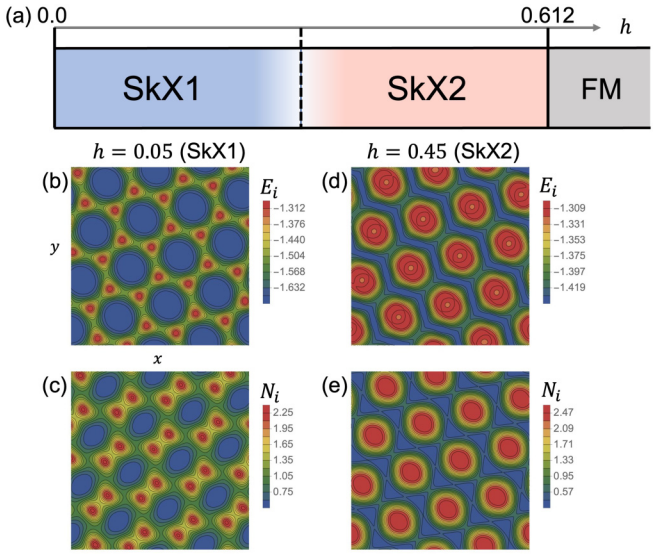

FIG. 1. Phase diagram showing typical skyrmion crystal configurations of SkX1 and SkX2 types. (b) and (d) show the energy density of SkX1 and SkX2, respectively, whereas (c) and (e) show the topological charge distribution. The simulations depicted here are made using 32^2 lattice sites.

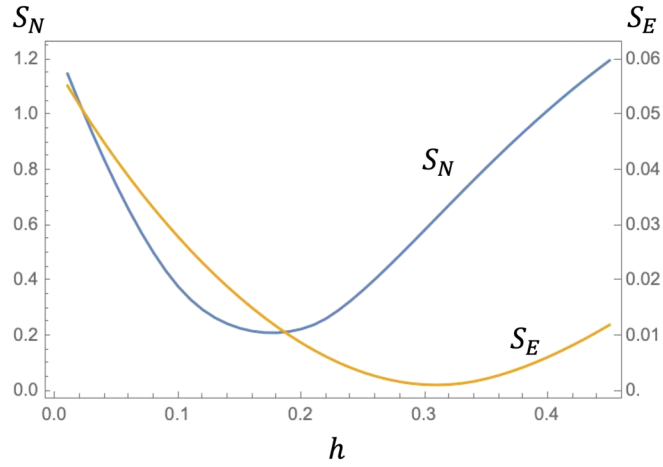

FIG. 2. Configurational entropy of the energy density S_E and topological charge density S_N.

III. $\mathbb{C}P^2$ SKYRMION CRYSTALS

We are now ready to explore skyrmion crystals in the model (7), which after fixing the parameters only possesses one free parameter, i.e., h. Varying h, we find three types of configurations: a skyrmion crystal of the first kind (SkX1), a skyrmion crystal of the second kind (SkX2), and the ferromagnetic state (FM) (see Fig. 1). We can see from the figure that SkX1 on a square lattice is almost a honeycomb lattice of half-skyrmions, whereas SkX2 consists of a triangular lattice of skyrmions with unit topological charge.

For convenience, we have subtracted off a constant from the energy so as to render the energy of the FM phase equal to zero. More precisely, we compute the energy as

$$E = H - \sum_i \left(\frac{4}{3}J - h\right), \tag{14}$$

with the Hamiltonian H. We determine the critical value of h for the phase transition to the FM phase by calculating the skyrmion energy. The critical value $h_{\text{crit}} \approx 0.612$ is the value of the Zeeman coupling for which the energy of the skyrmion becomes positive. On the other hand, SkX1 and SkX2 are connected via a crossover. In order to determine how they are distinguished, we propose to compute the configurational entropy (CE) of the energy and the topological charge densities, respectively [65–68]:

$$S_{E(N)} = -\sum_l f_{E(N)}(\mathbf{q}_l)\log f_{E(N)}(\mathbf{q}_l),$$
$$f_{E(N)}(\mathbf{q}_l) = \frac{|F_{E(N)}(\mathbf{q}_l)|^2}{\sum_i |F_{E(N)}(\mathbf{q}_i)|^2}. \tag{15}$$

Here, F_E and F_N are the discrete Fourier transform of the energy and topological charge densities, respectively, i.e., $F_{E(N)}(\mathbf{q}_l) = \mathcal{N}^{-1}\sum_j E_j(N_j)e^{i\mathbf{q}_l\cdot\mathbf{r}_j}$, where $\mathbf{q}_l$ is the momentum conjugate to $\mathbf{r}_l$ and $\mathcal{N}$ is the number of lattice sites. We show a plot of CE of the energy and topological charge density in Fig. 2.

We find that the minimum of the CE signals a change in the unit skyrmion's local structure. In particular, starting at small values of h, both the energy and topological charge densities have two peaks close to their respective minima. These two peaks break up into four peaks, which we may interpret as half-skyrmions becoming quarter-skyrmions in SkX2. This transition happens for smaller values of h for the topological charge density (viz., $h_{\text{crit}}^{\text{SkX1/2}} \approx 0.18$) as compared to the same happening for the energy density (viz., $h_{\text{crit}}^{\text{SkX1/2}} \approx 0.31$), see Fig. 2. Hence, there is not a clear-cut critical value of h for the transition between SkX1 and SkX2, but rather a range with a kind of crossover between the two $\mathbb{C}P^2$ skyrmion crystals.

We will now discuss some further properties of the skyrmion crystals (see Fig. 3 for the evolution of the two types of skyrmion crystals as functions of h, where the energy and topological charge densities are shown as the top and bottom rows of the figure). For the final properties, we define

$$\mathcal{X}(\mathbf{q}) = \mathcal{N}^{-2}\sum_{j,k}\langle\hat{\mathbf{X}}_j\rangle\cdot\langle\hat{\mathbf{X}}_k\rangle e^{i\mathbf{q}\cdot(\mathbf{r}_j-\mathbf{r}_k)}, \tag{16}$$

where $\mathcal{X} = \mathcal{S}$ (with $\hat{\mathbf{X}} = \hat{\mathbf{S}}$) is the dipole structure factor and $\mathcal{X} = \mathcal{Q}$ (with $\hat{\mathbf{X}} = \hat{\mathbf{Q}}$) is the quadrupole structure factor. Here, the expectation value of the quadrupole operator $\hat{\mathbf{Q}}_i$ is given by

$$\langle\hat{\mathbf{Q}}_i\rangle = \begin{pmatrix}\langle\hat{Q}_i^{x^2-y^2}\rangle\\ \langle\hat{Q}_i^{r^2-3z^2}\rangle\\ \langle\hat{Q}_i^{xy}\rangle\\ \langle\hat{Q}_i^{xz}\rangle\\ \langle\hat{Q}_i^{yz}\rangle\end{pmatrix} = \begin{pmatrix} n_i^4\\ \frac{\sqrt{3}n_i^3-n_i^8}{2}\\ n_i^5\\ \frac{n_i^1-n_i^6}{\sqrt{2}}\\ \frac{n_i^2-n_i^7}{\sqrt{2}}\end{pmatrix}, \tag{17}$$

where $\hat{Q}_i^{ab} = \hat{S}_i^a\hat{S}_i^b + \hat{S}_i^b\hat{S}_i^a - 4\delta_{ab}/3$ [41]. The middle of Fig. 4 shows the dipole structure factor $\mathcal{S}(\mathbf{q})$ and quadrupole structure factor $\mathcal{Q}(\mathbf{q})$. As usually observed in $\mathbb{C}P^1$ skyrmion crystals, $\mathcal{S}(\mathbf{q})$ shows the sharp peak at the Γ point and small triple-q structures with $|\mathbf{q}| \equiv q_S$ under a magnetic field. On

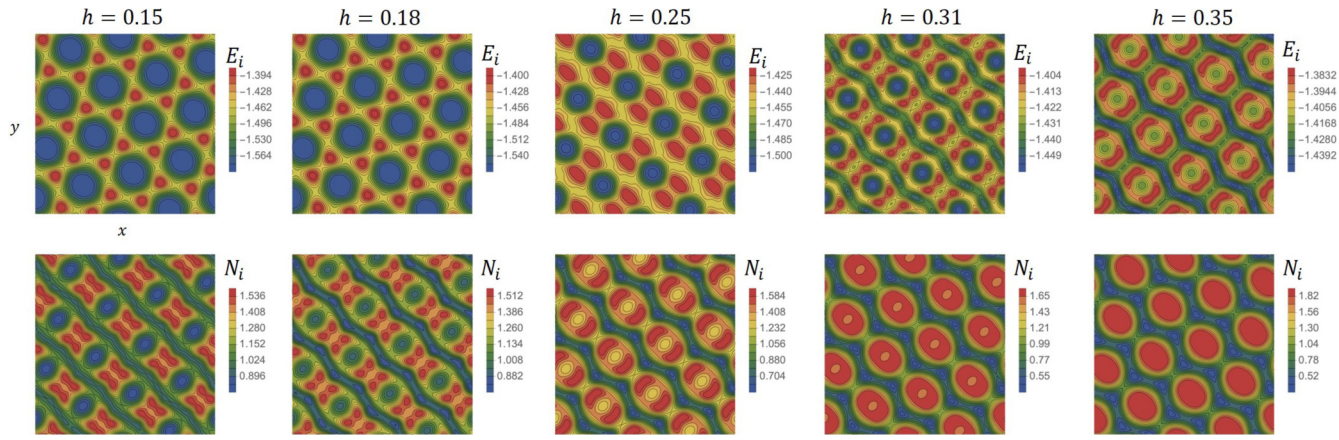

FIG. 3. The energy and topological charge densities of configurations for $h = 0.15$, 0.18, 0.25, 0.31, and 0.35. The upper panels represent the energy density and the lower ones show the topological charge density.

the other hand, as the characteristic feature of $\mathbb{C}P^2$ skyrmion crystals, sharp triple-q structures with $|\mathbf{q}| = q_S$ appear in $\mathcal{Q}(\mathbf{q})$. One can also see that SkX1 has a higher triple-q structure with $|\mathbf{q}| > q_S$ in $\mathcal{S}(\mathbf{q})$. Another difference between SkX1 and SkX2 is the position of higher triple-q peaks with $|\mathbf{q}| > q_S$ in $\mathcal{Q}(\mathbf{q})$.

Figure 4 also shows the magnetization vector as well as the toric $\mathbb{C}P^2$ diagram with the 2-cycle of the skyrmions charted out as white points. Since the 2-cycle is not concentrated on a single straight line on the toric $\mathbb{C}P^2$ diagram, we can see that the skyrmions are genuine $\mathbb{C}P^2$ skyrmions and not simply a $\mathbb{C}P^1$ skyrmion embedded into $\mathbb{C}P^2$. In SkX1, the magnetization vectors are longest at the core of fractional skyrmions and point in the $\hat{z}$ direction, whereas they have vanishing length in SkX2.

IV. CONCLUSION AND DISCUSSION

In this Letter, we have proposed the possibility of $\mathbb{C}P^2$ skyrmion crystals and have found two different types of crystals in an SU(3) spin system with Zeeman and the generalized DM terms as the stabilizing agent. To obtain additional information on the unit skyrmion's local structure, we have computed the configurational entropy of the energy and topological charge densities. Their minima correspond to bound states of two half-skyrmions and four quarter-skyrmions. As a characteristic feature of $\mathbb{C}P^2$ skyrmion crystals, we have found a triple-q structure in the quadrupole structure factors. Since $\mathbb{C}P^2$ skyrmions have more internal structures than $\mathbb{C}P^1$ skyrmions, it is of great interest to explore emergent phenomena in $\mathbb{C}P^2$ skyrmion crystals and consider their applications in future nanotechnology. In addition, we expect that $\mathbb{C}P^2$ skyrmion crystals are relevant even in high-energy physics, e.g., dense quark matter possessing SU(3) ferromagnetism [69].

While we have studied skyrmion crystals in a low-energy effective model of the simplest spin-1 Bose-Hubbard model with artificial gauge potentials and the Zeeman interaction, we expect that the skyrmion crystals survive even if we slightly introduce the spin-dependent interaction in the spin-1

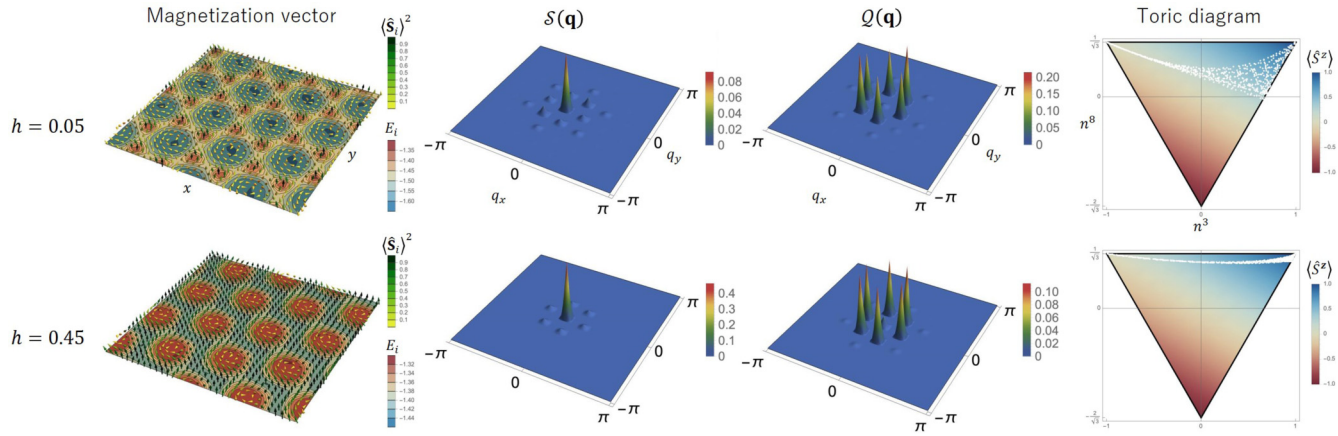

FIG. 4. Magnetization vector, dipole structure factor $\mathcal{S}(\mathbf{q})$, quadrupole structure factor $\mathcal{Q}(\mathbf{q})$, and configurational 2-cycle of the skyrmions shown on the toric diagram of $\mathbb{C}P^2$. The upper panels show the case of SkX1 with h chosen as $h = 0.05$, and the lower panels show SkX2 with $h = 0.45$. The color of the magnetic vectors illustrates their length, whereas the background color corresponds to the energy density. The color of the toric diagram represents instead the value of the third spin-1 component, i.e., $\langle \hat{S}^z \rangle = (n^3 + \sqrt{3}n^8)/2$.

Bose-Hubbard model that appears in the system of spinor BECs [70,71]. To show this, is the most important future problem. While we have considered the linear Zeeman term, the quadratic Zeeman term splits even a singly isolated skyrmion into fractional skyrmions (merons) [72], and thus investigating a skyrmion crystal with the quadratic Zeeman term would be an interesting future direction of research. It is also of great interest to consider skyrmion crystals appearing in a pseudospin system, i.e., a mixture of three species of bosons [73]. Other interesting directions are to investigate the properties at finite temperature [52,74–76] and to study skyrmion crystals in the antiferromagnetic SU(3) Heisenberg model with a generalized DM interaction, of which the continuum counterpart is a nonlinear sigma model on the flag manifold $SU(3)/U(1)^2$ [47,77–80].

Note added. Recently, we became aware of Ref. [81], which has some overlap with our results, in particular, the proposal to realize $\mathbb{C}P^2$ skyrmion crystals, albeit in different physical systems. In particular, while Ref. [81] utilizes frustration to stabilize the skyrmions, we considered the generalized DM interaction on a square lattice.

ACKNOWLEDGMENTS

The authors would like to thank N. Sawado for useful discussions. The work of Y. Akagi is supported by JSPS KAKENHI Grant No. JP20K14411 and JSPS Grant-in-Aid for Scientific Research on Innovative Areas "Quantum Liquid Crystals" (KAKENHI Grants No. JP20H05154 and No. JP22H04469). S.B.G. thanks the Outstanding Talent Program of Henan University and the Ministry of Education of Henan Province for partial support. The work of S.B.G. is supported by the National Natural Science Foundation of China (Grants No. 11675223 and No. 12071111). The work of M.N. is supported in part by JSPS Grant-in-Aid for Scientific Research (KAKENHI Grants No. JP18H01217 and No. JP22H01221). The computations in this paper were run on the "GOVORUN" cluster supported by the LIT, JINR.

[1] T. H. R. Skyrme, Nucl. Phys. **31**, 556 (1962).
[2] E. Witten, Nucl. Phys. B **223**, 433 (1983).
[3] N. Manton, *Skyrmions - A Theory of Nuclei* (World Scientific, Singapore, 2022).
[4] *The Multifaceted Skyrmions*, edited by M. Rho and I. Zahed, 2nd ed. (World Scientific, Singapore, 2016).
[5] A. A. Bogolubskaya and I. L. Bogolubsky, Phys. Lett. A **136**, 485 (1989).
[6] A. A. Bogolubskaya and I. L. Bogolubsky, Lett. Math. Phys. **19**, 171 (1990).
[7] B. M. A. G. Piette, B. J. Schroers, and W. J. Zakrzewski, Z. Phys. C **65**, 165 (1995).
[8] A. Bogdanov and D. Yablonskii, Sov. Phys. JETP **68**, 101 (1989).
[9] A. Bogdanov, JETP Lett. **62**, 247 (1995).
[10] S. Mühlbauer, B. Binz, F. Jonietz, C. Pfleiderer, A. Rosch, A. Neubauer, R. Georgii, and P. Böni, Science **323**, 915 (2009).
[11] X. Z. Yu, Y. Onose, N. Kanazawa, J. H. Park, J. H. Han, Y. Matsui, N. Nagaosa, and Y. Tokura, Nature (London) **465**, 901 (2010).
[12] S. Heinze, K. von Bergmann, M. Menzel, J. Brede, A. Kubetzka, R. Wiesendanger, G. Bihlmayer, and S. Blügel, Nat. Phys. **7**, 713 (2011).
[13] T. Kurumaji, T. Nakajima, M. Hirschberger, A. Kikkawa, Y. Yamasaki, H. Sagayama, H. Nakao, Y. Taguchi, T.-h. Arima, and Y. Tokura, Science **365**, 914 (2019).
[14] M. Hirschberger, T. Nakajima, S. Gao, L. Peng, A. Kikkawa, T. Kurumaji, M. Kriener, Y. Yamasaki, H. Sagayama, H. Nakao, K. Ohishi, K. Kakurai, Y. Taguchi, X. Yu, T.-h. Arima, and Y. Tokura, Nat. Commun. **10**, 5831 (2019).
[15] N. D. Khanh, T. Nakajima, X. Yu, S. Gao, K. Shibata, M. Hirschberger, Y. Yamasaki, H. Sagayama, H. Nakao, L. Peng, K. Nakajima, R. Takagi, T.-h. Arima, Y. Tokura, and S. Seki, Nat. Nanotechnol. **15**, 444 (2020).
[16] Y. Yasui, C. J. Butler, N. D. Khanh, S. Hayami, T. Nomoto, T. Hanaguri, Y. Motome, R. Arita, T.-h. Arima, Y. Tokura, and S. Seki, Nat. Commun. **11**, 5925 (2020).
[17] A. Fert, V. Cros, and J. Sampaio, Nat. Nanotechnol. **8**, 152 (2013).
[18] N. Nagaosa and Y. Tokura, Nat. Nanotechnol. **8**, 899 (2013).
[19] T. Okubo, S. Chung, and H. Kawamura, Phys. Rev. Lett. **108**, 017206 (2012).
[20] A. O. Leonov and M. Mostovoy, Nat. Commun. **6**, 8275 (2015).
[21] D. Amoroso, P. Barone, and S. Picozzi, Nat. Commun. **11**, 5784 (2020).
[22] Y. Akagi, M. Udagawa, and Y. Motome, Phys. Rev. Lett. **108**, 096401 (2012).
[23] R. Ozawa, S. Hayami, and Y. Motome, Phys. Rev. Lett. **118**, 147205 (2017).
[24] S. Hayami, R. Ozawa, and Y. Motome, Phys. Rev. B **95**, 224424 (2017).
[25] H. Eichenherr, Nucl. Phys. B **146**, 215 (1978); **155**, 544(E) (1979).
[26] V. L. Golo and A. M. Perelomov, Phys. Lett. B **79**, 112 (1978).
[27] E. Cremmer and J. Scherk, Phys. Lett. B **74**, 341 (1978).
[28] A. D'Adda, M. Luscher, and P. Di Vecchia, Nucl. Phys. B **146**, 63 (1978).
[29] E. Witten, Nucl. Phys. B **149**, 285 (1979).
[30] T. Senthil, A. Vishwanath, L. Balents, S. Sachdev, and M. P. A. Fisher, Science **303**, 1490 (2004).
[31] F. S. Nogueira and A. Sudbø, Europhys. Lett. **104**, 56004 (2013).
[32] C. Laflamme, W. Evans, M. Dalmonte, U. Gerber, H. Mejia-Diaz, W. Bietenholz, U. J. Wiese, and P. Zoller, Ann. Phys. **370**, 117 (2016).
[33] J. Garaud, J. Carlström, and E. Babaev, Phys. Rev. Lett. **107**, 197001 (2011).
[34] J. Garaud, J. Carlström, E. Babaev, and M. Speight, Phys. Rev. B **87**, 014507 (2013).
[35] A. Benfenati, M. Barkman, and E. Babaev, arXiv:2204.05242.
[36] N. Papanicolaou, Nucl. Phys. B **305**, 367 (1988).
[37] C. D. Batista and G. Ortiz, Adv. Phys. **53**, 1 (2004).
[38] H. Tsunetsugu and M. Arikawa, J. Phys. Soc. Jpn. **75**, 083701 (2006).

[39] A. Läuchli, F. Mila, and K. Penc, Phys. Rev. Lett. **97**, 087205 (2006).

[40] T. A. Tóth, A. M. Läuchli, F. Mila, and K. Penc, Phys. Rev. Lett. **105**, 265301 (2010).

[41] K. Penc and A. M. Läuchli, in *Introduction to Frustrated Magnetism: Materials, Experiments, Theory*, edited by C. Lacroix, P. Mendels, and F. Mila, Springer Series in Solid-State Sciences (Springer, Berlin, 2011), Vol. 164, p. 331.

[42] B. Bauer, P. Corboz, A. M. Läuchli, L. Messio, K. Penc, M. Troyer, and F. Mila, Phys. Rev. B **85**, 125116 (2012).

[43] B. A. Ivanov and A. K. Kolezhuk, Phys. Rev. B **68**, 052401 (2003).

[44] B. A. Ivanov and R. S. Khymyn, J. Exp. Theor. Phys. **104**, 307 (2007).

[45] B. A. Ivanov, R. S. Khymyn, and A. K. Kolezhuk, Phys. Rev. Lett. **100**, 047203 (2008).

[46] E. G. Galkina, B. A. Ivanov, O. A. Kosmachev, and Y. A. Fridman, Low Temp. Phys. **41**, 382 (2015).

[47] H. T. Ueda, Y. Akagi, and N. Shannon, Phys. Rev. A **93**, 021606(R) (2016).

[48] J. Takano and H. Tsunetsugu, J. Phys. Soc. Jpn. **80**, 094707 (2011).

[49] T. Grover and T. Senthil, Phys. Rev. Lett. **107**, 077203 (2011).

[50] C. Xu and A. W. W. Ludwig, Phys. Rev. Lett. **108**, 047202 (2012).

[51] S. Hu, A. M. Turner, K. Penc, and F. Pollmann, Phys. Rev. Lett. **113**, 027202 (2014).

[52] K. Remund, R. Pohle, Y. Akagi, J. Romhányi, and N. Shannon, Phys. Rev. Res. **4**, 033106 (2022).

[53] A. Imambekov, M. Lukin, and E. Demler, Phys. Rev. A **68**, 063602 (2003).

[54] G. Juzeliūnas, J. Ruseckas, and J. Dalibard, Phys. Rev. A **81**, 053403 (2010).

[55] J. Dalibard, F. Gerbier, G. Juzeliunas, and P. Ohberg, Rev. Mod. Phys. **83**, 1523 (2011).

[56] N. Goldman, G. Juzeliūnas, P. Öhberg, and I. B. Spielman, Rep. Prog. Phys. **77**, 126401 (2014).

[57] H. Zhai, Rep. Prog. Phys. **78**, 026001 (2015).

[58] Stabilization of three-dimensional skyrmions in ultracold atomic gases with an SOC was proposed in Ref. [82].

[59] I. R. Klebanov, Nucl. Phys. B **262**, 133 (1985).

[60] M. Kugler and S. Shtrikman, Phys. Rev. D **40**, 3421 (1989).

[61] B.-Y. Park and D. O. Riska, Skyrmion approach to finite density and temperature, in *The Multifaceted Skyrmions* (Ref. [4]), Chap. 7, pp. 131–162.

[62] See Supplemental Material at http://link.aps.org/supplemental/10.1103/PhysRevB.106.L100406 for a derivation of the model from the spin-1 Bose-Hubbard model, using the Schrieffer-Wolff transformation, which includes Refs. [83–86].

[63] Y. Akagi, Y. Amari, N. Sawado, and Y. Shnir, Phys. Rev. D **103**, 065008 (2021).

[64] It may still be an experimental challenge to control the DM term in two (spatial) dimensions.

[65] M. Gleiser and N. Stamatopoulos, Phys. Lett. B **713**, 304 (2012).

[66] M. Gleiser and D. Sowinski, Phys. Lett. B **747**, 125 (2015).

[67] D. Bazeia, D. Moreira, and E. Rodrigues, J. Magn. Magn. Mater. **475**, 734 (2019).

[68] D. Bazeia and E. Rodrigues, Phys. Lett. A **392**, 127170 (2021).

[69] M. Kobayashi, E. Nakano, and M. Nitta, J. High Energy Phys. 06 (2014) 130.

[70] D. M. Stamper-Kurn and M. Ueda, Rev. Mod. Phys. **85**, 1191 (2013).

[71] Y. Kawaguchi and M. Ueda, Phys. Rep. **520**, 253 (2012).

[72] Y. Akagi, Y. Amari, S. B. Gudnason, M. Nitta, and Y. Shnir, J. High Energy Phys. 11 (2021) 194.

[73] T. Graß, R. W. Chhajlany, C. A. Muschik, and M. Lewenstein, Phys. Rev. B **90**, 195127 (2014).

[74] E. M. Stoudenmire, S. Trebst, and L. Balents, Phys. Rev. B **79**, 214436 (2009).

[75] D. Yamamoto, C. Suzuki, G. Marmorini, S. Okazaki, and N. Furukawa, Phys. Rev. Lett. **125**, 057204 (2020).

[76] K. Tanaka and C. Hotta, Phys. Rev. B **102**, 140401(R) (2020).

[77] Y. Amari and N. Sawado, Phys. Rev. D **97**, 065012 (2018).

[78] Y. Amari and N. Sawado, Phys. Lett. B **784**, 294 (2018).

[79] I. Affleck, D. Bykov, and K. Wamer, Phys. Rep. **953**, 1 (2022).

[80] I. Takahashi and Y. Tanizaki, Phys. Rev. B **104**, 235152 (2021).

[81] H. Zhang, Z. Wang, D. Dahlbom, K. Barros, and C. D. Batista, arXiv:2203.15248.

[82] T. Kawakami, T. Mizushima, M. Nitta, and K. Machida, Phys. Rev. Lett. **109**, 015301 (2012).

[83] J. R. Schrieffer and P. A. Wolff, Phys. Rev. **149**, 491 (1966).

[84] T. Barthel, C. Kasztelan, I. P. McCulloch, and U. Schollwöck, Phys. Rev. A **79**, 053627 (2009).

[85] S. Zhu, Y.-Q. Li, and C. D. Batista, Phys. Rev. B **90**, 195107 (2014).

[86] J. H. Pixley, W. S. Cole, I. B. Spielman, M. Rizzi, and S. Das Sarma, Phys. Rev. A **96**, 043622 (2017).